

ChemComm

Chemical Communications

Accepted Manuscript

This article can be cited before page numbers have been issued, to do this please use: T. Neal, J. Cao, B. Luzel, Y. Guillaneuf and J. Nicolas, *Chem. Commun.*, 2026, DOI: 10.1039/D6CC03260E.



This is an Accepted Manuscript, which has been through the Royal Society of Chemistry peer review process and has been accepted for publication.

Accepted Manuscripts are published online shortly after acceptance, before technical editing, formatting and proof reading. Using this free service, authors can make their results available to the community, in citable form, before we publish the edited article. We will replace this Accepted Manuscript with the edited and formatted Advance Article as soon as it is available.

You can find more information about Accepted Manuscripts in the [Information for Authors](#).

Please note that technical editing may introduce minor changes to the text and/or graphics, which may alter content. The journal's standard [Terms & Conditions](#) and the [Ethical guidelines](#) still apply. In no event shall the Royal Society of Chemistry be held responsible for any errors or omissions in this Accepted Manuscript or any consequences arising from the use of any information it contains.

COMMUNICATION

POT-PISA: Core-degradable particles via aqueous radical ring-opening polymerisation-induced self-assembly using 7-phenyloxepane-2-thioneThomas J. Neal,^a Jingming Cao,^a Bastien Luzel,^b Yohann Guillaneuf,^b and Julien Nicolas^{a,*}Received 00th January 20xx,
Accepted 00th January 20xx

DOI: 10.1039/x0xx00000x

We report the successful synthesis of novel core-degradable nanoparticles using 7-phenyloxepane-2-thione (POT) via an aqueous radical ring-opening polymerisation-induced self-assembly process. These nanoparticles efficiently degrade in the presence of amines, demonstrating a molar mass reduction of the core by up to 85%.

There is a significant drive to create degradable vinyl polymers for biomedical applications to ensure and facilitate the safe excretion of the material.¹ This desire is further motivated by environmental issues surrounding plastics and their end-of-life disposal (*e.g.* plastic pollution and microplastics).^{2–4} In light of this, there is a renewed interest in radical ring-opening copolymerisation (rROP) as a method for producing degradable vinyl polymers *via* the integration of cleavable bonds into the copolymer backbone.^{5–7} Recently, thionolactones have been shown to copolymerise with a range of vinyl monomers *via* a thiocarbonyl-addition-ring opening (TARO) mechanism, integrating labile thioester groups into the copolymer backbone.^{8–10} Recently we, and others, have reported the rROP of the thionolactone, dibenzo[*c,e*]oxepane-5-thione (DOT) with industrially relevant isoprene (I), biomedically important *N*-isopropylacrylamide (NIPAAm) and acrylamide (AAm) as well as the conventional emulsion copolymerisation with *n*-butylacrylate (BA) and styrene (St).^{6,11–13}

Additionally, thiolactones have been integrated into aqueous nanoparticles through polymerisation-induced self-assembly (PISA), through a rROPISA process.^{14,15} Galanopoulo *et al.* recently reported the extension of hydrophilic poly(*N*-acryloylmorpholine) (PNAM) with DOT and either BA or St *via* reversible addition-fragmentation chain-transfer (RAFT) aqueous emulsion copolymerisation to form core-degradable spherical nanoparticles.¹⁴ This work demonstrated that PISA can be utilised to form aqueous polymeric nanoparticles that display excellent core-degradability under basic conditions. Furthermore, we recently reported the first example of DOT-

containing degradable vesicles synthesised via aqueous rROPISA. This synthesis utilised a monomer-starved methodology to ensure an even distribution of DOT in the vesicle membrane, resulting in significant degradability. Such higher order morphologies are relevant in a multitude of biomedical applications such as in drug encapsulation and delivery.^{16–21}

Although DOT has been shown to be an efficient comonomer for the integration of degradable moieties, it has some drawbacks in terms of reactivity.¹⁰ DOT is known to efficiently copolymerise with acrylate derivatives but has a low reactivity with styrene. This limitation can be overcome by performing the copolymerisation at higher temperatures (150 °C) and in bulk.¹⁰ However, performing the copolymerisation at 80 °C leads to poor incorporation of DOT. Recently, DFT calculations were used to discover a new thionolactone with better statistical comonomer incorporation. This work led to the development of 7-phenyloxepane-2-thione (POT), a thionolactone that copolymerises well with both styrene and acrylate derivatives to produce statistical copolymers.²²

Herein, to expand the versatility and applicability of the rROPISA process, we report the integration of POT into a RAFT-mediated aqueous rROPISA system to produce sterically stabilised, core-degradable, diblock copolymer nanoparticles (Fig. 1). Specifically, we demonstrate the copolymerisation of POT with both BA and St using hydrophilic poly(dimethylacrylamide) (PDMA) as a steric stabiliser. This formulation yields nanoparticles that can degrade under basic conditions. This work describes the first demonstration of RAFT-mediated rROPISA system using POT as a thionolactone comonomer.

A PDMA macro-CTA (**PDMA-CTA**) was synthesised via the RAFT solution polymerisation of dimethylacrylamide (DMA) in dioxane (Fig. 1). The reaction was quenched by exposure to air after 4 h and a monomer conversion of 75%. This reaction was stopped prior to 100% monomer conversion in an attempt to preserve the RAFT chain-ends of the PDMA homopolymer, as the trithiocarbonate group of the RAFT agent is susceptible to

^a Université Paris-Saclay, CNRS, Institut Galien Paris-Saclay, 17 avenue des Sciences 91400 Orsay, France. Email: julien.nicolas@universite-paris-saclay.fr

^b Aix-Marseille Université, CNRS, Institut de Chimie Radicale, UMR 7273, F-13397 Marseille, France.



hydrolysis at high monomer conversion.²³ This **PDMA-CTA** (Table 1) was isolated and purified by precipitation and any

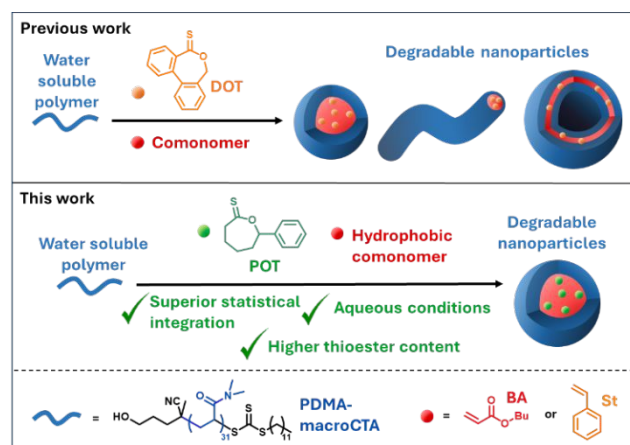


Fig. 1 Schematic representation of the context for the present study.

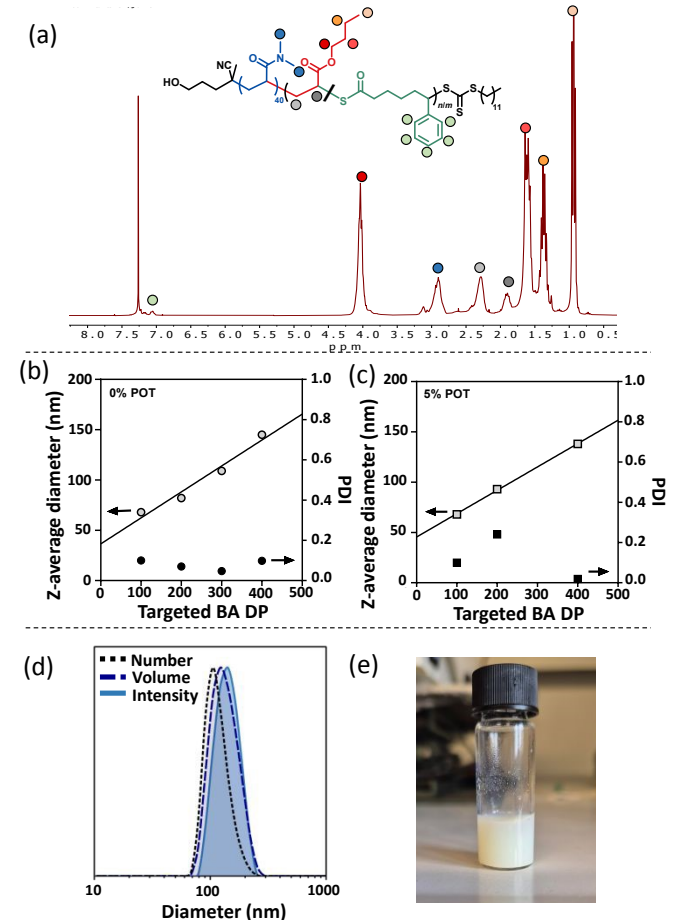
residual solvent was removed under reduced pressure. The number-average degree of polymerisation (DP_n) was calculated to be 31 (which equates to a number-average molar mass, M_n , of 3.4 kDa) by ^1H NMR spectroscopy using the integrals of the CH_3 of the RAFT chain-end and the $(\text{CH}_3)_2$ of DMA. Additionally, the M_n of the **PDMA-CTA** was determined by SEC in DMSO. It was found to be 3.2 kDa, with a narrow dispersity (M_w/M_n) of 1.09 relative to pullulan standards, which is concordant with the M_n estimated by ^1H NMR spectroscopy.

Sterically stabilised block copolymer nanoparticles were synthesised by extension of the **PDMA-CTA** with BA and 5 mol% POT ($f_{\text{POT},0} = 0.05$), via aqueous emulsion rROPISA (Fig. 1, Table 1). The target DP of the core forming block was systematically varied from 105 to 420 (copolymers **2**, **5**, and **7**). Nanoparticles without the presence of POT were additionally synthesised as a reference (copolymers **1**, **3**, **4**, and **6**). The size of the resultant nanoparticles was assessed by DLS. A linear increase in particle size with increasing core DP was observed in both the presence and absence of POT (Figure 2b and c). Furthermore, a homogeneous size distribution was observed for all the nanoparticles (Figure 2d). Additionally, it was found that the presence of POT had little effect on the particle size. For example, copolymer **1** ($f_{\text{POT},0} = 0$) and **2** ($f_{\text{POT},0} = 0.05$) had a Z-average diameter of 145 nm and 138 nm, respectively.

^1H NMR spectroscopy was performed on lyophilised dispersions to determine the POT content in the final copolymer (F_{POT}) (Fig. 2a). By comparing the POT aromatic proton resonances with the CH_2 resonance of PBA, the copolymer composition could be obtained. The calculated F_{POT} was consistently higher than the initial POT feed ratio ($f_{\text{POT},0}$), suggesting good incorporation of the thionolactone comonomer. Furthermore, the F_{POT} was calculated to be as high as 0.07, which is significantly higher than has been obtained for equivalent DOT dispersions.^{15,24}

The M_n of the copolymers were determined by SEC in chloroform and compared to narrow poly(methyl methacrylate) (PMMA) standards (Table 1). As expected, a significantly larger M_n was observed after the extension with BA and POT. Despite

this increase in M_n , the presence of a small peak at 14.8 min indicates that 100% blocking efficiency was not achieved and



some unreacted macro-CTA remains (Fig. 3a, b and S2).

Fig. 2 (a) ^1H NMR spectrum of copolymer **2** showing the presence of POT. Evolution of the particle average diameter and polydispersity with targeted DP_{BA} , with either: (b) $f_{\text{POT}} = 0$ or (c) $f_{\text{POT}} = 0.05$, where (d) is an example of normalised size distribution for the intensity averaged particle diameter (copolymer **2**). (e) Digital image of the copolymer nanoparticles **2**.

As previously mentioned, the Z-average diameter was not significantly affected by the presence of POT in the copolymer backbone, however, the apparent M_n was affected. Comparing systems with and without POT as a comonomer indicates that the integration of POT leads to a reduction in the observed molar mass – this observation is particularly evident at high DPs (e.g., comparison of copolymer **1** and **2**, Table 1). However, comparable M_n s are observed for block copolymers with smaller core DPs (ca. DP = 100), such as copolymers **7** (5% POT) and **6** (0% POT) that have a M_n s of 39.8 kDa and 38.2 kDa, respectively. Furthermore, in the case where no POT is integrated into the particle core, relatively narrow molar mass distribution was achieved ($M_w/M_n < 1.4$). However, it was found that, in general, M_w/M_n increased when POT was copolymerised with BA ($M_w/M_n < 1.55$). This observation is more pronounced when targeting higher molar masses. For example, a broader distribution was observed for copolymer **2** ($M_w/M_n = 1.55$, DP = 420) than for copolymers **5** ($M_w/M_n = 1.32$, DP = 210) and **7** ($M_w/M_n = 1.31$, DP = 105). These results suggest that the presence of POT affects the RAFT control and is particularly affected at lower concentrations of RAFT chain-end.



Table 1. Experimental conditions for the synthesis of PDMA-*b*-P(BA-*co*-POT) and PDMA-*b*-P(St-*co*-POT) copolymer particles by aqueous emulsion rROPISA and their macromolecular characteristics and degradation behaviour.

Sample	Macro-CTA	M/POT/RAFT/I	M	$f_{\text{POT},0}$	M_n (kDa) ^a	\bar{D} ^a	F_{POT}	M_n (kDa) ^{a,b}	$\bar{D}^{a,b}$
PDMA-CTA	-	40/0/1/0.2	DMA	0.00	3.2 ^c	1.09	-	-	-
1	PDMA ₃₁	400/0/1/0.5	BA	0.00	94.5	1.35	-	-	-
2	PDMA ₃₁	400/20/1/0.5	BA	0.05	44.4	1.55	0.07	11.0	1.56
3	PDMA ₃₁	300/0/1/0.5	BA	0.00	80.7	1.23	-	-	-
4	PDMA ₃₁	200/0/1/0.5	BA	0.00	57.1	1.44	-	-	-
5	PDMA ₃₁	200/10/1/0.5	BA	0.05	47.0	1.32	0.07	10.3	1.52
6	PDMA ₃₁	100/0/1/0.5	BA	0.00	38.2	1.32	-	-	-
7	PDMA ₃₁	100/5/1/0.5	BA	0.05	39.8	1.31	0.06	8.7	2.23
8	PDMA ₃₁	200/0/1/0.5	St	0.00	42.6	1.20	-	-	-
9	PDMA ₃₁	400/10/1/0.5	St	0.02	53.1	1.23	n.d. ^d	50.9	1.24
10	PDMA ₃₁	400/20/1/1	St	0.05	37.4	1.54	n.d. ^d	36.2	1.52
11^f	PDMA ₃₁	400/20/1/1	St	0.05	15.3	1.45	n.d. ^d	8.1 ^e	1.56 ^e

^a Number-average molar mass measured by chloroform SEC against PMMA standards. ^b Measured after 24 h in the presence of isopropylamine. ^c Number-average molar mass measured by DMSO SEC against Pullulan standards. ^d Not determined due to overlapping signals in the ¹H NMR spectrum. ^e Measured after 24 h in the presence of ethanolamine, similar results also observed using butylamine. ^f Monomer-starved synthesis.

Aqueous degradation studies were performed on copolymer nanoparticles **2**, **5**, and **7**, whose targeted core DP were 105, 210, and 420, respectively. Degradation was initiated by the addition isopropylamine (iPrNH₂), which has been previously shown to induce aminolysis of the backbone thioester.^{6,15,24} After 24 h, the reaction was quenched by neutralisation with acetic acid and lyophilised prior to SEC analysis. A substantial decrease in M_n was observed for all the samples after degradation. For example, the M_n of copolymer **5** reduced from 47 kDa to 10 kDa (78% loss). Similarly, a M_n loss of 75% and 78% was observed for copolymers **2** and **7**, respectively. Taking into consideration the non-degradable PDMA segment these values increase to 81%, 84%, and 85% for copolymers **2**, **5**, and **7**, respectively. The maximum theoretical M_n reduction for the degradable block can be calculated based upon the mole fraction of POT present in the copolymer chain using the assumption that a relatively even distribution of POT has been achieved along the copolymer backbone. Accordingly, the maximum loss for copolymers **2**, **5**, and **7**, were calculated to be 86–88%. The astounding concordance between the experimental results and the theoretical values confirm that a significant amount of POT is present in the particle core and demonstrate that the degradation of these nanoparticles can be performed easily and efficiently in aqueous media.

Using a similar protocol, extension of **PDMA-CTA** with St and POT ($f_{\text{POT}} = 0.02$) was performed via aqueous emulsion PISA (Fig. 1, copolymer **9**, Table 1). Compared with BA, the polymerisation of St was much slower and often required an increased amount of initiator in order to reach high monomer conversion. This was particularly evident in the presence of POT and often very low monomer conversions of St would be observed in 24 h. To account for this, a 1:1 ratio of **PDMA-CTA** to initiator was used. Despite the high levels of initiator, relatively narrow dispersities were achieved for these copolymers ($M_w/M_n < 1.55$). As was the case for the PBA series, residual macro-CTA can be observed in the SEC chromatogram at a retention time of 14.8 min

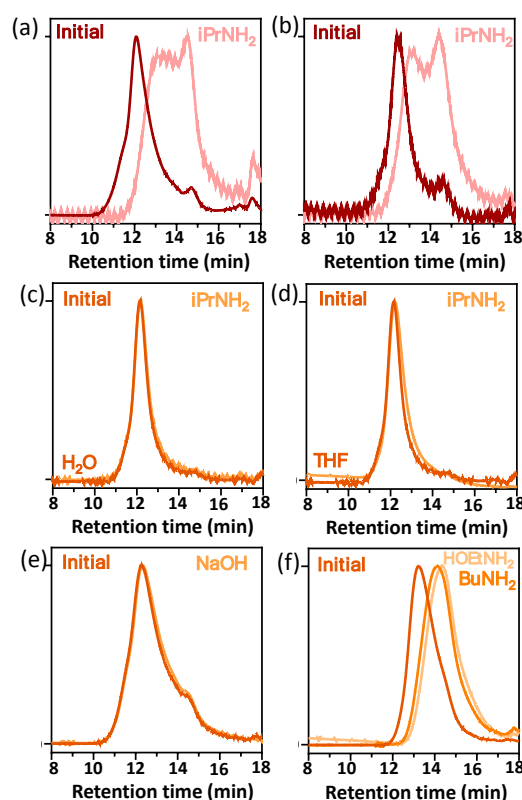


Figure 3. Evolution of the SEC RI-chromatograms of PDMA-*b*-P(BA-*co*-POT) copolymers: (a) **2**, (b) **7**, (c) **9** in H₂O, (d) **9** in THF, (e) **10**, and (f) **11** (Table 1), before and after degradation under aminolytic and basic conditions.

indicating less than 100% blocking efficiency (Figure 3c). Similarly to the PBA nanoparticles, stable nanoparticles were formed (Z -average diameter = 120 nm, PDI = 0.105).

Initial aqueous degradation studies were performed on copolymer nanoparticle **9** by the addition of iPrNH₂. Conversely, to the PBA series, no significant decrease in M_n was observed after 24 h (Figure 3c). Additionally, no degradation was observed in organic solvent where the copolymer was fully dissolved (Figure 3d). These results suggested that no, or too



little amount of POT had been integrated into the copolymer backbone.

In an attempt to integrate POT into the copolymer backbone, the POT content within the monomer feed was increased from $f_{\text{POT}} = 0.02$ to 0.05 (copolymer **10**, Table 1). Although the apparent synthesis of these nanoparticles was successful no degradation was observed in the presence of NaOH for 24 h (Figure 3e), suggesting again that no significant amount of POT has been integrated into the copolymer. It is worth noting that identification of the presence of POT by ^1H NMR spectroscopy was not possible due to the overlapping of POT peaks with the aromatic resonances of PSt. However, other techniques (e.g. quantitative ^{13}C NMR spectroscopy) could be explored in future studies for determination of POT content.

Finally, a monomer-starved synthesis of these nanoparticles were attempted, where a POT/St (5:95) mixture was slowly added to the heated aqueous solution of PDMA-CTA and initiator over the course of 4 h (copolymer **11**). Monomer-starved methods have shown promise in similar systems, resulting in an even distribution and integration of DOT into the core of PISA nanoparticles.¹⁵ Here, this method produced stable nanoparticles. However, full monomer conversion was not achieved – this is apparent from the low M_n observed by SEC (Table 1, Figure 3f) and can be due to a lower in-situ monomer concentration resulting in a lower propagation rate. Nonetheless, aqueous degradation was attempted in the presence of less bulky amines e.g., butylamine (BuNH_2) and ethanolamine (HOEtNH_2), as it has been previously shown that reaction of sterically hindered amines is less favourable due to the rigid and bulky structure of PSt.^{25,26} Interestingly, a significant decrease in M_n was observed after 24 h, confirming the presence of POT in the copolymer backbone. The M_n decreased from 15 kDa to 8 kDa (47% decrease) and 6 kDa (60% decrease) for BuNH_2 and HOEtNH_2 , respectively.

In conclusion, a series of PBA/POT block copolymer particles stabilised by PDMA were synthesised at different molecular weights. The high POT content achieved in these formulations allowed efficient degradation of the particle core in the presence of $i\text{PrNH}_2$ after 24 h – achieving up to 85% molar mass loss, which is extremely comparable to the theoretical maximum for these systems. However, the synthesis of PSt/POT particles was not successful using the same one-pot procedure, as no degradation was observed in the presence of $i\text{PrNH}_2$ in aqueous and organic conditions or using NaOH. It was therefore concluded that POT was not integrated into the copolymer backbone. An alternative monomer-starved method proved successful at integrating POT into the backbone as evidenced by significant reduction of M_n in the presence of amines. This work identifies POT as an efficient comonomer to establish degradability in vinyl copolymer particles, achieving higher degradability than the previously reported DOT systems. Furthermore, this work establishes a precedent for further exploration of thionolactone systems and their integration into PISA formulations. As has been shown previously, such degradable nanoparticles have high interest in biomedical application,¹¹ such as in drug delivery, warranting continued investigation.

View Article Online
DOI: 10.1039/D6CC03260E

Conflicts of interest

There are no conflicts to declare.

Data availability

The data supporting this article is included as part of the ESI.

Notes and references

This work was supported by the Bettencourt Schueller Foundation. CNRS and University Paris-Saclay are also acknowledged for funding.

- 1 V. Delplace and J. Nicolas, *Nature Chem*, 2015, **7**, 771–784.
- 2 G. Sen, in *Plastic Pollution: Challenges and Green Solutions*, eds. M. Goel and N. G. Tripathi, Springer Nature Singapore, Singapore, 2024, pp. 139–157.
- 3 A. T. Williams and N. Rangel-Buitrago, *Marine Pollution Bulletin*, 2022, **176**, 113429.
- 4 M. MacLeod, H. P. H. Arp, M. B. Tekman and A. Jahnke, *Science*, 2021, **373**, 61–65.
- 5 A. Tardy, J. Nicolas, D. Giges, C. Lefay and Y. Guillaeneuf, *Chem. Rev.*, 2017, **117**, 1319–1406.
- 6 T. J. Neal and J. Nicolas, *Chem. Commun.*, 2024, **60**, 14260–14263.
- 7 T. Pesenti and J. Nicolas, *ACS Macro Lett.*, 2020, **9**, 1812–1835.
- 8 N. M. Bingham and P. J. Roth, *Chem. Commun.*, 2019, **55**, 55–58.
- 9 R. A. Smith, G. Fu, O. McAteer, M. Xu and W. R. Gutekunst, *J. Am. Chem. Soc.*, 2019, **141**, 1446–1451.
- 10 N. Gil, B. Caron, D. Siri, J. Roche, S. Hadiouch, D. Khedaioui, S. Ranque, C. Cassagne, D. Montarnal, D. Giges, C. Lefay and Y. Guillaeneuf, *Macromolecules*, 2022, **55**, 6680–6694.
- 11 M. Lages, T. Pesenti, C. Zhu, D. Le, J. Mougin, Y. Guillaeneuf and J. Nicolas, *Chem. Sci.*, 2023, **14**, 3311–3325.
- 12 N. M. Bingham, Q. U. Nisa, S. H. L. Chua, L. Fontugne, M. P. Spick and P. J. Roth, *ACS Appl. Polym. Mater.*, 2020, **2**, 3440–3449.
- 13 M. Lages, N. Gil, P. Galanopoulou, J. Mougin, C. Lefay, Y. Guillaeneuf, M. Lansalot, F. D'Agosto and J. Nicolas, *Macromolecules*, 2022, **55**, 9790–9801.
- 14 P. Galanopoulou, N. Gil, D. Giges, C. Lefay, Y. Guillaeneuf, M. Lages, J. Nicolas, F. D'Agosto and M. Lansalot, *Angew Chem Int Ed*, 2023, **62**, e202302093.
- 15 P. G. Georgiou, T. J. Neal, M. A. Newell, K. S. Hepburn, J. J. S. Tyler, M. A. H. Farmer, P. Chohan, P. J. Roth, J. Nicolas and S. P. Armes, *J. Am. Chem. Soc.*, 2025, **147**, 19817–19828.
- 16 X. Zhao, C. Sun, F. Xiong, T. Wang, S. Li, F. Huo and X. Yao, *Research*, 2023, **6**, 0113.
- 17 C. Hua and L. Qiu, *IJN*, 2024, **Volume 19**, 2317–2340.
- 18 A. Czajka, S. J. Byard and S. P. Armes, *Chem. Sci.*, 2022, **13**, 9569–9579.
- 19 S. E. Ahmed, N. L. Fletcher, A. R. Prior, P. Huda, C. A. Bell and K. J. Thurecht, *Polym. Chem.*, 2022, **13**, 4004–4017.
- 20 J. Lefley, C. Waldron and C. R. Becer, *Polym. Chem.*, 2020, **11**, 7124–7136.
- 21 N. Grimaldi, F. Andrade, N. Segovia, L. Ferrer-Tasies, S. Sala, J. Veciana and N. Ventosa, *Chem. Soc. Rev.*, 2016, **45**, 6520–6545.



- 22 B. Luzel, N. Gil, P. Désirée, J. Monot, D. Bourissou, D. Siri, D. Gimes, B. Martin-Vaca, C. Lefay and Y. Guillauneuf, *J. Am. Chem. Soc.*, 2023, **145**, 27437–27449.
- 23 C. Boyer, V. Bulmus and T. P. Davis, *Macromol. Rapid Commun.*, 2009, **30**, 493–497.
- 24 P. Galanopoulo, N. Gil, D. Gimes, C. Lefay, Y. Guillauneuf, M. Lages, J. Nicolas, F. D'Agosto and M. Lansalot, *Angew Chem Int Ed*, 2023, **62**, e202302093.
- 25 K. Fuji, Y. Kitayama and A. Harada, *ACS Appl. Polym. Mater.*, 2025, **7**, 3349–3357.
- 26 P. Galanopoulo, N. Gil, D. Gimes, C. Lefay, Y. Guillauneuf, M. Lages, J. Nicolas, M. Lansalot and F. D'Agosto, *Angew Chem Int Ed*, 2022, **61**, e202117498.

View Article Online
DOI: 10.1039/D6CC03260E



Data availability

The data supporting this article is included as part of the ESI.

